Original Investigation | CLINICAL SCIENCES

Early-Onset Foveal Involvement in Retinitis Punctata Albescens With Mutations in *RLBP1*

Elodie Dessalces, BS, EBOD; Béatrice Bocquet, PhD; Jérôme Bourien, PhD; Xavier Zanlonghi, MD; Robert Verdet, MD; Isabelle Meunier, MD, PhD; Christian P. Hamel, MD, PhD

IMPORTANCE Retinitis punctata albescens (RPA) is an autosomal recessive form of retinitis pigmentosa characterized by white dotlike deposits in the fundus, in most cases caused by mutations in *RLBP1*.

OBJECTIVE To study disease progression and visual function in RPA.

DESIGN We performed clinical and molecular investigations in patients with RPA at various ages, from November 5, 2003, through June 20, 2012, with no planned patient follow-up.

SETTING The National Reference Center for Genetic Sensory Diseases (Montpellier).

PARTICIPANTS Eleven patients with RPA (mean age, 24 [range, 3-39] years) from 7 families and 11 control subjects undergoing evaluation.

EXPOSURE Optical coherence tomography measurements.

MAIN OUTCOMES AND MEASURES Screening for mutations by polymerase chain reaction sequencing of the 9 *RLBP1* exons. Patients underwent standard ophthalmic examination, fundus imaging, autofluorescence testing, Goldmann visual field measurement, optical coherence tomography, adaptive optics–based infrared fundus ophthalmoscopy, dark adaptometry, and electroretinography.

RESULTS We found 2 novel *RLBP1* mutations (p.Tyr111X and p.Arg9Cys), and 8 patients from Morocco were homozygous for the recurrent 7.36-kilobase *RLBP1* deletion of exons 7 through 9. All patients had night blindness (before age 6 years in 10). The dotlike deposits were generally dense but could be rare, appearing in adaptive optics as elongated structures with variable orientation and no foveal involvement. We found no specific refractive error, and visual acuity varied widely from normal (1.2) to counting fingers. Variable degrees of visual field impairment were present, and all patients had severely decreased electroretinographic responses with predominant rod impairment. No correlation between visual acuity ($P = .27$) or visual field and age ($P = .08$) was present. On optical coherence tomography, the mean (SD) central foveal (122 [23] vs 187 [30] μm in controls) and foveal (147 [19] vs 217 [17] μm) thicknesses were significantly ($P < .01$) decreased, independently of age, whereas the retinal thickness at the 3- and 6-mm rings around the fovea progressively decreased with age. Mean (SD) cone number was normal in 1 patient aged 13 years (21 000/mm^2 [2000/mm^2]) but dropped to 10 500/mm^2 (5244/mm^2), 8667/mm^2 (2944/mm^2), and 5833/mm^2 (983/mm^2) in 3 other patients aged 39, 32, and 29 years, respectively.

CONCLUSIONS AND RELEVANCE Patients with RPA show variable degrees of foveal cone death, even at an early stage. This finding has implications for future treatment.

JAMA Ophthalmol. 2013;131(10):1314-1323. doi:10.1001/jamaophthalmol.2013.4476
Published online August 8, 2013.

Author Affiliations: Author affiliations are listed at the end of this article.

Corresponding Author: Christian P. Hamel, MD, PhD, Institut des Neurosciences de Montpellier, Institut National de la Santé et de la Recherche Médicale U1051, Hôpital Saint-Eloi, BP 74103, 80 rue Augustin Fliche, 34091 Montpellier, CEDEX 05, France (christian.hamel@inserm.fr).

Retinitis punctata albescens (RPA) is a subtype of autosomal recessive retinitis pigmentosa (RP) featuring characteristic glistening, small white dotlike spots more or less covering the major part of the fundus. In 1910, Lauber[1(p133)] proposed that among flecked retinae, RPA, a progressive retinal degeneration, should be distinguished from the "fundus albipunctatus cum hemeralopia," which was stationary. Retinitis punctata albescens was reported as a nonsyndromic retinal degeneration, but it was occasionally found in association with lenticonus,[2] Friedreich ataxia,[3] Senior-Loken syndrome,[4] Bardet-Biedl syndrome,[5] and congenital sensorineural deafness.[6] Therefore, the term *RPA* may be applied to distinct forms of retinal dystrophies and, as such, appeared to be a descriptive pattern rather than a disease. However, when mutations were discovered in *RLBP1*,[7-9] RPA was clearly identified as a particular clinical and genetic entity. Mutations in *RLBP1* were also found in 2 geographically restricted areas in clinical forms of RPA, that is, the Bothnia retinal dystrophy[8] and Newfoundland rod-cone dystrophy.[10] Most RPA cases are simplex or multiplex, corresponding to the autosomal recessive inheritance, but the condition has been rarely reported in association with autosomal dominant RP.[11-13] Retinitis punctata albescens might account for 0.5% of all RP cases or 1% of autosomal recessive and sporadic RP.[14] Assuming that RP prevalence is 1 in 4000 in developed countries,[15] RPA would therefore have an approximate prevalence of 1 in 800 000.

Retinitis punctata albescens is considered a rod-cone dystrophy type of RP that typically features early childhood-onset night blindness. The fundus of patients with RPA shows the other signs of RP, including narrowing of the retinal vessels, pigment deposits, and retinal atrophy. Nevertheless, subtle differences are found with the typical RP features. At the middle stage of evolution (approximately before 40 years of age), narrowing of the retinal vessels remains rather moderate compared with RP, and the pallor of the optic disc is absent or mild.[10,16,17] In addition, bone spiculelike pigment deposits are rare or even absent. The visual field is usually normal in childhood and adolescence, but in the late teenage years paracentral scotomas may appear, which later enlarge centrally and toward the periphery. Characteristically, large atrophic spots (best seen in autofluorescent funduscopy or fluorescein angiography) appear progressively in the midperipheral retina with few pigment deposits and fewer white punctuations. Macular involvement is frequent, usually as a progressive macular atrophy, but macular cystoid edema can also be found. Dark adaptation is always abnormal and electroretinographic (ERG) recordings are highly depressed, impairing more rod than cone responses.

The *RLBP1* gene encodes the cellular retinaldehyde-binding protein, a key actor of the visual cycle that binds 11-*cis*-retinol produced by the consecutive action of lecithin retinol acyltransferase (LRAT) and the isomerohydrolase RPE65 in the retinal pigment epithelium.[18,19] Also, RPA shares some clinical features with retinal dystrophies caused by *RPE65* or *LRAT* mutations.[20-22] Because recent clinical trials in *RPE65* or *LRAT* conditions have shown that gene therapy or pharmacological treatments could partially restore visual functions,[23-25] such therapeutic approaches might also benefit patients with RPA. In this study, we examined a large series of patients with RPA and *RLBP1* mutations, many of them carrying the recurrent exon 7 through 9 deletion.[26] We show that, although the disease progression is slow, a variable degree of foveal cone death occurs, even at an early stage.

Methods

Patients

We included 11 patients belonging to 7 families, of whom 5 families originated from Morocco (MTP702, MTP1554, MTP1633, MTP1789, and MTP1838) and 2 from France (MTP857 and MTP1254). The study has authorization from the French Ministry of Health for biomedical research in the field of physiology, pathophysiology, epidemiology, and genetics in ophthalmology (11018S). Informed and written consent was obtained for all patients participating in the study. The investigators followed the tenets of the Declaration of Helsinki.

Clinical Investigations

Patients underwent the standard ophthalmologic examination (refractometry, visual acuity, slitlamp examination, applanation tonometry, and funduscopy). Kinetic visual fields were determined with a Goldmann perimeter with targets V-4-e, III-4-e, and I-4-e. Optical coherence tomography (OCT) measurement of the macula was performed using a third-generation OCT system (Stratus model 3000; Carl Zeiss Meditec) with the manufacturer's software (version 3.0). Central foveal thickness (minimal foveal thickness), foveal thickness (ring diameter, 1 mm), and the superior, inferior, temporal, and nasal areas of inner (ring diameter, 3 mm) and outer (ring diameter, 6 mm) rings were measured. Autofluorescence measurements were obtained with a retinal confocal angiograph (Heidelberg Retina Angiograph II; Heidelberg Engineering), and fundus images were obtained. Full-field ERGs were recorded using a Ganzfeld apparatus (Metrovision) with a bipolar contact lens electrode on maximally dilated pupils according to the protocol of the International Society for Clinical Electrophysiology of Vision.[27] Cone mosaic investigation was performed by adaptive optics-based infrared fundus ophthalmoscopy (AOIO) with a retinal camera (RTX-1; Imagine Eyes).

For numerical values, visual acuity was measured with Snellen charts in decimal numbers. Goldmann visual field was quantified by counting the number of subdivisions of the Goldmann grid within the areas of the V-4-e isopter and expressed as a percentage of the normal visual field. Correlations between visual variables (visual acuity, visual field, OCT retinal thickness, and ERG amplitudes) and age were investigated with the Pearson correlation coefficient. Cone number was manually counted on 3 parafoveal spots per eye, each covering 1000 μm^2, and the mean (SD) cone number per square micrometer was calculated.

Molecular Investigations

Informed consent and blood samples were obtained from the patients. Genomic DNA was extracted from 10-mL peripheral blood samples by a standard salting out procedure[28] and stored

Figure 1. Pedigrees of 7 Families With Retinitis Punctata Albescens and *RLBP1* Mutations

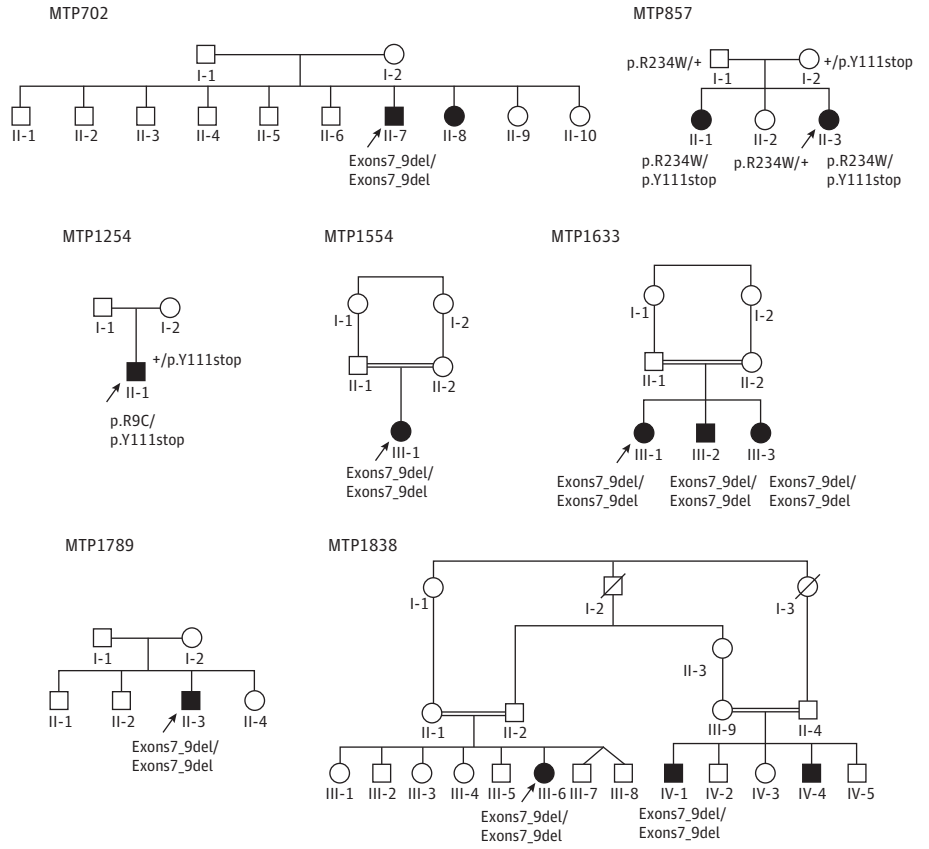

Squares indicate male; circles, female; and plus sign, wild-type allele. Blackened symbols are individuals affected with retinitis punctata albescens. A double horizontal line between the mating pair indicates consanguinity, and black arrows, probands. The patient numbers show the generation in roman numerals and the order in the generation in arabic numbers. The genotype of the tested patients is indicated.

at −20°C before use. Exons 1 through 9 of the *RLBP1* gene and intronic flanking regions (GenBank NG_008116) were amplified with polymerase chain reaction in a 25-µL reaction mix containing 50 ng of genomic DNA, 0.2µM solutions of each primer (available on request), 1.5mM (fragments 1 and 3) or 2.5mM (fragments 2 and 4) magnesium chloride, 200µM deoxyribonucleotide triphosphates, and 0.25 U of *Taq* polymerase (Invitrogen) in its appropriate buffer. After the first denaturation at 94°C for 3 minutes, amplification was performed in 35 cycles at 94°C for 30 seconds, 58°C for 40 seconds, and 72°C for 45 seconds, ending with a final extension step for 7 minutes. The polymerase chain reaction products were purified with a cleaning product (ExoSAP-it; Amersham Biosciences). Sequencing of all amplified fragments was performed using a cycle sequencing reaction kit (BigDye Terminator version, 3.1; Applied Biosystems) on a capillary electrophoresis DNA sequencer (ABI PRISM 3130; Applied Biosystems). Sequencing results were analyzed using the manufacturer's software (SeqScape, version 2.5; Applied Biosystems).

Results

Identification of *RLBP1* Mutations in Patients With RPA

The 8 patients from the 5 families from Morocco were all homozygous for the recurrent *RLBP1* deletion of exons 7 through 9 (**Figure 1**). The 2 sisters of family MTP857 were compound heterozygous for the recurrent *RLBP1* mutation c.700C>T (p.Arg234Trp) encountered in Bothnia dystrophy and a novel mutation c.333T>G in exon 5 (p.Tyr111X). The simplex case of family MTP1254 was compound heterozygous for the same novel mutation (p.Tyr111X) and another novel mutation c.25C>T in exon 4 (p.Arg9Cys) that was absent from 112 control chromosomes (Figure 1).

Clinical Findings in Patients With RPA

Clinical findings are summarized in **Table 1**. Mean age at initial examination for this study was 24 (range, 3-39) years. All patients had night blindness. This symptom was the earliest to appear; it was always present in the medical history in 5 of 11 patients and noted to have begun between 2 and 6 years of age in the other 6 patients. Photophobia was present in 7 of 11 patients, and the sense of impaired visual field was only noticed by 2 patients at the adult stage. No specific refractive error was noted because the mean spherical equivalent was +0.11 (range, +3.25 to −5.375) diopters. Visual acuity varied widely from normal (1.2) to counting fingers. None of the patients had cataract.

Funduscopy revealed the characteristic white dotlike deposits at the level of the outer retina (**Table 2**). The deposits were generally dense and distributed more or less evenly over the posterior pole and in the midperiphery (**Figure 2**A and B),

Table 1. Summary of Clinical Features

Family (Patient/Age, y)	Night Blindness/ Age, y[a]	Photophobia/ Age, y[a]	Peripheral Vision Impairment/ Age, y[a]	OD		OS	
				Refraction[b]	Visual Acuity	Refraction[b]	Visual Acuity, LogMAR
MTP702 (II-7/31)	Yes/6	Yes/ND	Yes/ND	+1.00 (−0.50; 90°)	CF, 1 m	+1.25 (−1.00; 105°)	CF, 1 m
MTP857 (II-3/27)	Yes/2	No	No	+3.50 (−0.75; 170°)	CF, 1 m	+3.75 (−1.00; 40°)	0.4
MTP857 (II-1/32)	Yes/AP	Yes/ND	No	+0.25 (−2.00; 25°)	0.4	−0.25 (−1.25; 180°)	0.8
MTP1254 (II-1/13)	Yes/5	Yes/12	No	+1.75 (−3.50; 175°)	1.2	+1.25 (−4.00; 180°)	1.0
MTP1633 (III-1/39)	Yes/AP	Yes/AP	No	+1.00 (−1.50; 15°)	0.8	+1.00 (−1.25; 135°)	1.0
MTP1633 (III-2/32)	Yes/AP	Yes/AP	No	(−2.25; 5°)[c]	0.3	−0.50 (−2.00; 180°)	0.3
MTP1633 (III-3/29)	Yes/AP	Yes/AP	No	−4.00 (−2.75; 10°)	0.5	−3.50 (−1.50; 150°)	0.8
MTP1554 (III-1/4)	Yes/3	No	No	+3.25 (−0.75; 15°)	0.5	+2.75 (−0.75; 10°)	0.5
MTP1789 (II-3/3)	Yes/2	No	No	+3.50 (−0.50; 175°)	0.8	+3.50 (−0.50; 15°)	0.8
MTP1838 (III-6/22)	Yes/AP	No	No	−2.25 (−2.50; 15°)	0.7	−1.25 (−2.50; 155°)	0.7
MTP1838 (IV-1/33)	Yes/3	Yes/14	Yes/22	+2.50 (−1.50; 165°)	0.05	+2.00 (−1.75; 175°)	0.05

Abbreviations: AP, always present by medical history; CF, counting fingers; ND, not determined; OD, right eye; OS, left eye.

[a] Indicates apparent age at onset.

[b] The number before the parentheses is the value in diopters of the sphere correction, the first number in parentheses is the value in diopters of the cylinder, and the second number in parentheses indicates the axis of the cylinder.

[c] This patient had no sphere defect.

Table 2. Summary of Funduscopy Findings

Family (Patient)	Fundus			
	White Dots	Macula	Vessel Attenuation	Pigment Deposits
MTP702 (II-7)	Dense, unevenly distributed in periphery, present in macular area	R eye: macular atrophy; L eye: foveal atrophy	Moderate	No
MTP857 (II-3)	Rare, only in L eye along the temporal vascular arcades	R eye: severe atrophy; L eye: abnormal foveal reflex	Moderate	Rare (midperiphery)
MTP857 (II-1)	Dense, unevenly distributed in periphery, present in macular area, not in fovea	In each eye: abnormal foveal reflex	Slight	No
MTP1254 (II-1)	Dense, unevenly distributed in periphery, present in macular area, not in fovea	In each eye: abnormal foveal reflex	No	No
MTP1633 (III-1)	Dense, distributed evenly and radially in periphery, present in macular area, not in fovea	In each eye: Abnormal foveal reflex	Moderate	Rare (midperiphery)
MTP1633 (III-2)	Very dense, distributed evenly and radially in periphery, present in macular area, not in fovea	In each eye: Slightly discolored fovea	Moderate	No
MTP1633 (III-3)	Very dense, distributed evenly and radially in periphery, present in macular area, not in fovea	In each eye: Abnormal foveal reflex	Moderate	No
MTP1554 (III-1)	Dense, unevenly distributed in periphery, not in macular area	Normal macula	No	No
MTP1789 (II-3)	Dense, unevenly distributed in periphery, present in macular area, not in fovea	In each eye: Abnormal foveal reflex	Slight	No
MTP1838 (III-6)	Very dense, unevenly distributed in periphery, present in macular area, not in fovea	In each eye: Abnormal foveal reflex	Moderate	No
MTP1838 (IV-1)	Rare, unevenly distributed in macular area	In each eye: Perifoveal yellow ring	Moderate	Many (midperiphery), atrophic patches

Abbreviations: L, left; R, right.

including the macular area but sparing the fovea (Figure 2C). In family MTP1633, all 3 affected siblings showed a similar radial distribution of very dense white dots (Figure 2A). Conversely, in family MTP857, the older sister (II-1) had many dots (Figure 2D), whereas the younger sister (II-3) had none except for a few in the left eye along the temporal superior vascular arcade (Figure 2E and F). Fundus autofluorescence showed discrete hypoautofluorescent spots that overlapped only partially with the white dots, suggesting a masking effect of the retinal pigment epithelial autofluorescence (Figure 2J and K [insets]). In some patients, a slightly heterogeneous increase in autofluorescence was found, but magnification did not re-

Figure 2. Fundus Images of Patients With Retinitis Punctata Albescens

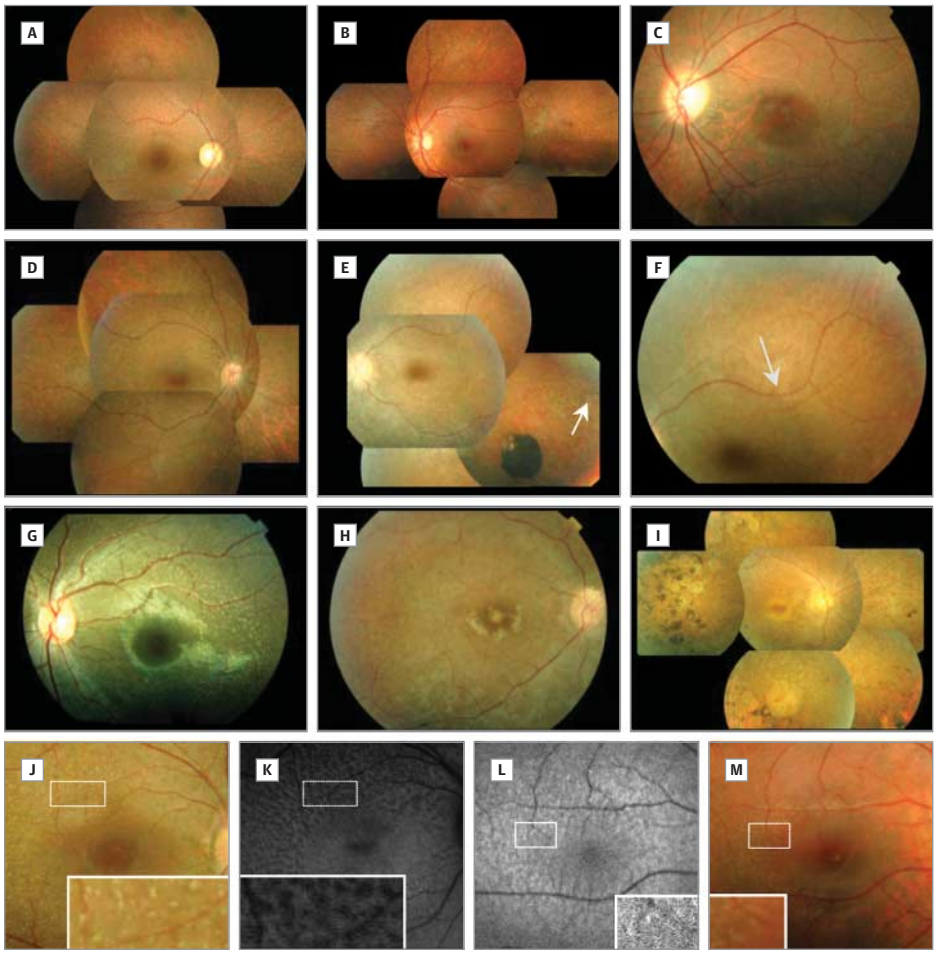

Pedigrees for each patient are given in Figure 1. A and B, Patient III-2 from family MTP1633 and patient II-1 from family MTP1254, respectively, show widespread white dotlike deposits throughout the fundus. C, Patient III-6 from family MTP1838 shows foveal sparing of the white deposits. D, Patient II-1 from family MTP857 has widespread white deposits. E, Patient II-3 from family MTP857 has only a few bone spicule-shaped pigment deposits (arrow). F, The same patient has a few white deposits on the superior temporal vascular arcade area of the left eye (arrow). G, Patient II-3 from family MTP1789 has an abnormal foveal reflex. H, Patient II-3 from family MTP857 has foveal and perifoveal atrophy. I, Patient IV-1 from family MTP1838 has an advanced disease stage with scallop-shaped peripheral atrophic spots containing pigment deposits, foveal atrophy, a moderately pale optic disc, and narrowing of the retinal vessels. J and K, A color photograph and autofluorescence, respectively, of the macular area in patient II-1 from family MTP857. Insets show magnification of spots of decreased autofluorescence that do not exactly correspond to white dotlike deposits. L and M, Autofluorescence and a color photograph, respectively, of the macular area in patient II-1 from family MTP1254. Insets show magnification of heterogeneous autofluorescence and white dotlike deposits in part M that are not localized in part L.

veal overlap with the white punctuations (Figure 2L and M [insets]). Pigment deposits were rare (Figure 2E) but were encountered more frequently in advanced disease stages in which scallop-shaped peripheral atrophic spots also became visible (Figure 2I). The optic disc appeared well preserved in all examined cases, and vascular attenuation was variable.

All patients had macular changes on funduscopy, ranging from abnormal foveal reflex (Figure 2G) to atrophy (Figure 2H), except for patient III-1 in family MTP1554, who was only 4 years of age. None of the patients had macular edema or cystic changes. However, OCT showed that all of them had significantly decreased mean (SD) retinal thickness in the central fovea (122 [23] vs 187 [30] µm in controls), the fovea (147 [19] vs 217 [17] µm), and 3-mm rings in all 4 quadrants ($P < .01$) (**Figure 3**). In addition, the retina was thinner in the fovea and in the 3- than in the 6-mm ring. The third high-reflectance band (HRB) representing the junction between the photoreceptor inner and outer segments was also abnormal in all patients except II-1 in family MTP1254. In 6 of 22 eyes, the third HRB was absent, and of these 5 eyes had the worse visual acuity (<0.05). Three eyes had a third HRB only present in the retrofoveal area, 11 of 22 eyes had a partially distinct HRB, and 2 eyes had an intact HRB (II-1 in family MTP1254).

No correlation was found between visual acuity and age ($P = .27$) (**Figure 4**A) or between central foveal ($P = .20$) and foveal ($P = .02$) thickness with age (Figure 4B), but the retinal thickness at the 3- and 6-mm rings significantly decreased with age ($P < .01$ for both rings and all quadrants), with correlation coefficients at 0.94, 0.90, 0.82, and 0.64 in

the 3-mm rings and 0.85, 0.76, 0.78, and 0.79 in the 6-mm rings for the superior, temporal, inferior, and nasal quadrants, respectively. The temporal side was the most affected quadrant (Figure 4B). We did not find any correlation between visual acuity and foveal thickness (P = .49).

Goldmann perimetry was performed in 9 of 11 patients (not applicable in the youngest patients) (**Table 3**). These patients retained a mean of 53.6% of the normal visual field (range, 15%-76%; age range, 13-39 years), with little difference between the central 10° (62%) and the field outside the central 10° (52%), indicating that the decrease in visual field occurred more or less simultaneously in the peripheral and central visual fields. Central scotoma was indeed evident in 5 of 9 cases. Central scotoma was associated with macular changes (patient II-7 in family MTP702, II-3 in family MTP857, III-2 and III-3 in family MTP1633, and IV-1 in family MTP1838) and decrease in visual acuity (except for patient III-3 in family MTP1633). We found no correlation between age and visual field (P = .08) (Figure 4C). Dark adaptometry was performed in 5 patients (age range, 13-39 years), and the findings were always abnormal, with an absolute threshold at 30 minutes raised 3.0 to 4.5 log U above reference values (mean, 3.8 log U).

Ten of the 11 patients underwent full-field ERG, which revealed decreased a- and b-wave amplitudes for rods and cones, with predominant rod impairment in all 10. Rod response amplitudes were severely decreased, ranging from undetectable to 13 µV, with 19 of 20 eyes below the limit of detection. Mixed rod-cone response amplitudes were similarly decreased, ranging from undetectable to 35 µV, with 12 of 20 eyes below the limit of detection (**Table 4**). Cone-specific 30-Hz flickers were delayed and showed less decreased amplitudes, with only 2 eyes from the same patient under the limit of detection, whereas 8 of 11 had at least 10 µV (2 patients had no flickers on ERG). Although the tendency was for 30-Hz flickers to decrease with age, no significant correlation between age and amplitude of 30-Hz flickers was evident (P = .06). Four patients (age range, 13-39 years) underwent 2-hour dark-adapted ERG. They all showed partial recovery of rod and rod-cone response amplitudes at 15% and 25% of the reference value, respectively. The youngest patient in this investigation (age 13 years) showed the best recovery, with 40% of the reference value for rod-cone responses.

Cone mosaic was analyzed with AOIO in parafoveal areas in 4 patients. The mean (SD) cone number (21 000/mm^2 [2000/mm^2]) in the youngest patient (II-1 in family RP1254; age 13 years) was within reference limits (**Figure 5**B), but the cone mosaic was slightly disorganized compared with that of a healthy individual (Figure 5A). However, in the 3 patients from family RP1633 (patients III-1 [age 39 years], III-2 [age 32 years], and III-3 [age 29 years]), the mean cone number dropped at 10 500/mm^2 (5244/mm^2), 8667/mm^2 (2944/mm^2), and 5833/mm^2 (983/mm^2), respectively. In addition, the cone mosaic was disorganized, with increased cone spacing and empty spaces (Figure 5C and D), especially above the elongated structures corresponding to the white dots (Figure 5E). Results of AOIO revealed the white dotlike deposits in the parafoveal area as elongated structures with variable orientation (Figure 5F) that were absent in the central foveal region (Figure 5G) compared with normal eyes (Figure 5H).

Figure 3. Retinal Thickness of the Macular Area of Patients With Retinitis Punctata Albescens

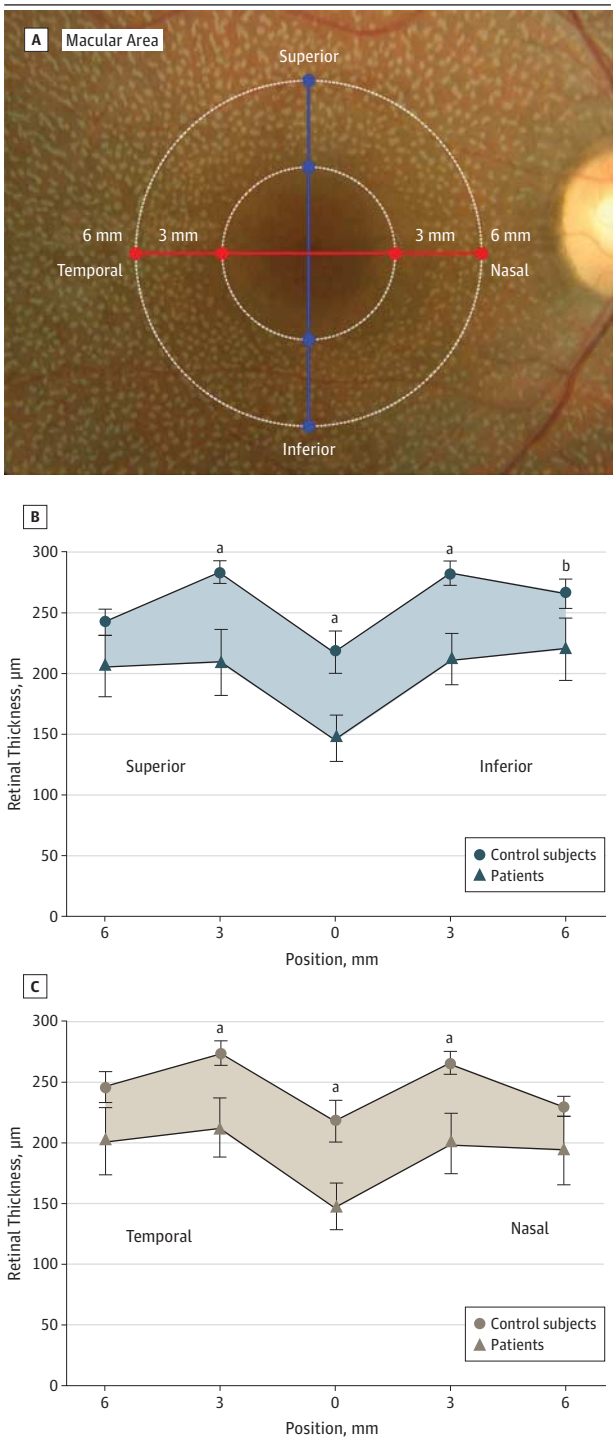

A, Fundus image indicates foveal thickness (crossing of the axes) and thickness at the inner (3-mm) and outer (6-mm) rings along the vertical and horizontal axes. B and C, Retinal thickness of the 22 eyes (11 patients) along the vertical and horizontal axes, respectively, compared with 22 eyes from 11 healthy control subjects shows significant differences at the fovea and 3-mm ring.
[a] P < .001.
[b] P < .01.

Figure 4. Visual Function of Patients With Retinitis Punctata Albescens as a Function of Age

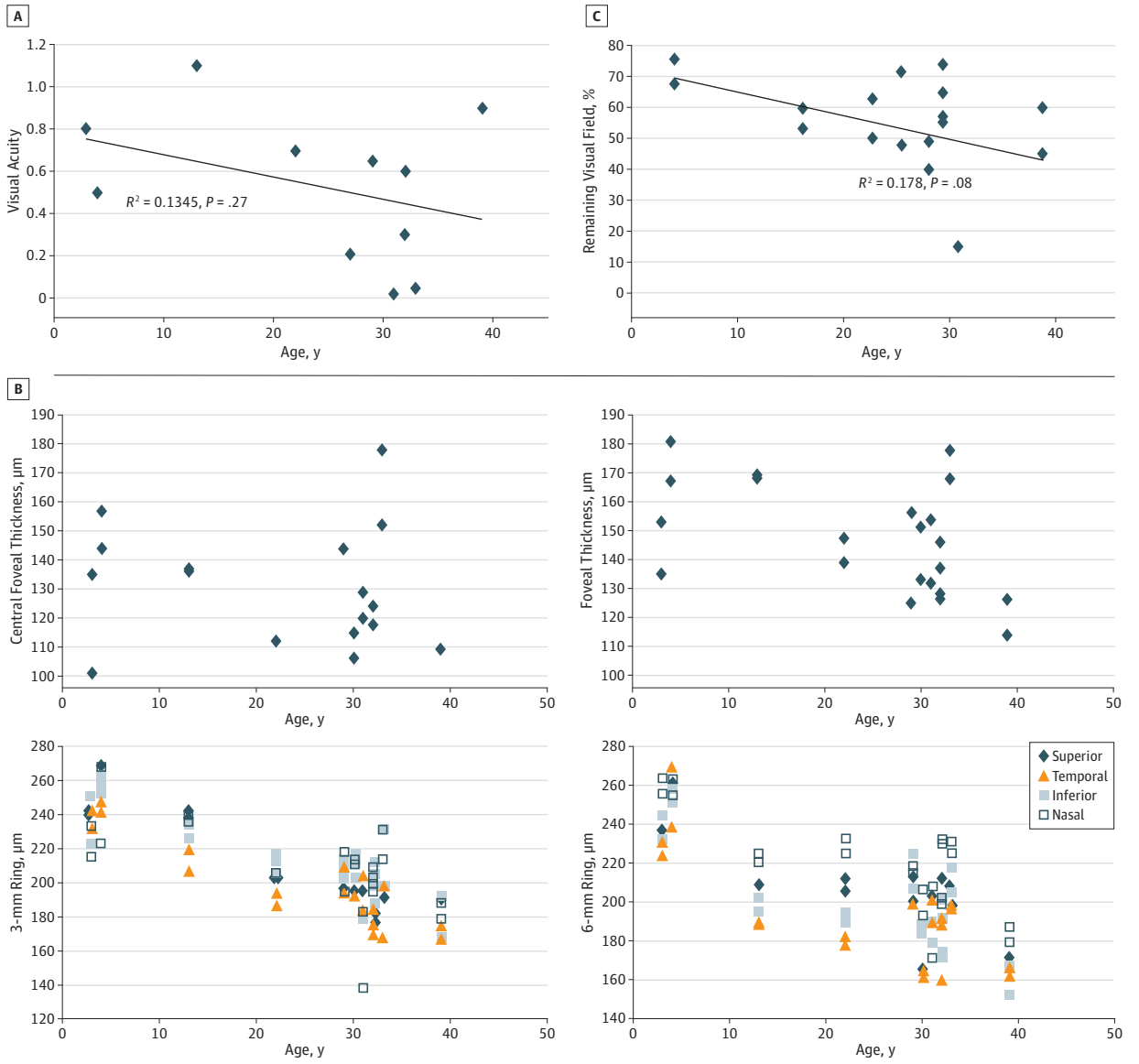

A, Mean visual acuity of both eyes of the 11 patients as a function of age. B, Retinal thickness of the 22 eyes (11 patients) was measured in the central fovea, in the fovea, and at the 3- and 6-mm rings in the superior, temporal, inferior, and nasal quadrants and plotted as a function of age. C, Percentage of the remaining visual field as determined by the Goldmann V-4-e isopter for 22 eyes as a function of age.

Discussion

In this study, 11 patients from 7 families with RPA underwent screening, which revealed biallelic mutations in *RLBP1*. Two novel *RLBP1* mutations were found, raising the number of mutations described for this gene to 13. The Tyr111Stop mutation, located in exon 5, probably causes the activation of the messenger RNA decay mechanism and therefore is a null allele. The Arg9Cys mutation is predicted to be damaging and has never been reported in databases, whereas an Arg9His change has been found in 2 of 12 996 cases of the exome variant server database. All the Moroccan patients carried the same previously described 7.36-kilobase deletion,[26] suggesting that these patients with RPA have inherited the mutated allele from a common ancestor.

All patients had RPA, although with some variations. Night blindness was the most prominent symptom and a constant finding, although rare cases have been reported with night blindness appearing in adulthood.[29] In contrast, most patients did not complain of impairment in their peripheral visual field, even at the young adult stage. Patients had moderate narrowing of the retinal vessels and optic nerve pallor, as well as rare pigment deposits, as are usually observed in RPA.[16,30] White dotlike deposits are characteristic features of the disease, and patients who had

Table 3. Results of Visual Field and Thickness Measurements

Family (Patient)	Goldmann Perimetry		Macular Findings	Foveal Thickness, μm[a]	
	R Eye	L Eye		R Eye	L Eye
MTP702 (II-7)	V-4-e 50°N, 80°T, 20° absolute CS	V-4-e 40°N, 40°T, 20° absolute CS	No IS/OS line in fovea broken in periphery	154	132
MTP857 (II-3)	V-4-e 40°N, 80°T, absolute CS	V-4-e 40°N, 65°T, T scotoma 15°-50°	R eye: foveal atrophy; L eye: IS/OS line in fovea only OS	133	151
MTP857 (II-1)	V-4-e 45°N, 60°T, T scotoma 20°-40°	V-4-e 50°N, 50°T	IS/OS line in fovea, broken in periphery	128	126
MTP1254 (II-1)	V-4-e 60°N, 80°T	V-4-e 50°N, 80°T	Conserved IS/OS line	169	168
MTP1633 (III-1)	V-4-e 35°N, 35°T	V-4-e 50°N, 45°T	R eye: no IS/OS line; L eye: broken IS/OS line	126	114
MTP1633 (III-2)	V-4-e 60°N, 90°T, 10° relative CS	V-4-e 60°N, 90°T, 10° relative CS	Broken IS/OS line	146	137
MTP1633 (III-3)	V-4-e 50°N, 80°T, 10° relative CS	V-4-e 50°N, 80°T, 10° relative CS	Broken IS/OS line	156	125
MTP1554 (III-1)	NP	NP	Slightly broken IS/OS line	167	181
MTP1789 (II-3)	NP	NP	Broken IS/OS line better in retrofovea	153	135
MTP1838 (III-6)	V-4-e 40°N, 50°T	V-4-e 40°N, 50°T	IS/OS line in fovea only	147	139
MTP1838 (IV-1)	50° Absolute CS, islands of vision	50° Absolute CS, islands of vision	Absent IS/OS line	168	178

Abbreviations: CS, central scotoma; IS/OS, inner segment/outer segment; L, left; N, nasal; NP, not performed; R, right; T, temporal.

[a] Foveal thickness is defined as the 1-mm central ring (reference range, 189-249 μm).

Table 4. Results of Full-Field ERG

Family (Patient)	Dark-Adapted b-Wave ERG, Dim Blue and Maximal Stimulation, μV[a]		10-min Light-Adapted ERG With 30-Hz Flickers, μV[b]	Dark Adaptometry, Absolute Threshold
	20-min	2-h		
MTP702 (II-7)	<10; <10	NP	NP	Raised 4 log U at 30 min
MTP857 (II-3)	<10; <10	NP	20	NP
MTP857 (II-1)	<10; 10	NP	12	NP
MTP1254 (II-1)	<10 to 13; 35	60; 115-140	80	Raised 3 log U at 30 min
MTP1633 (III-1)	<10; <10	20; 37-45	10-15	Raised 4.5 log U at 30 min
MTP1633 (III-2)	<10; <10	35-40; 55	10-13	Raised 3.5 log U at 30 min
MTP1633 (III-3)	<10; 15-20	<10; 31-40	16-22	Raised 4 log U at 30 min
MTP1554 (III-1)	NP	NP	NP	NP
MTP1789 (II-3)	<10; <10	NP	34	NP
MTP1838 (III-6)	<10; 15	NP	15	NP
MTP1838 (IV-1)	<10; <10	NP	<10	NP

Abbreviations: ERG, electroretinography; NP, not performed.

[a] Reference value for dim blue value is 165 μV or greater; for maximal stimulation, 250 μV or greater.

[b] Reference value is 100 μV or greater; ranges indicate range between the left and right eyes.

them were selected for *RLBP1* screening. However, the presence of the white dotlike deposits could be an inconstant finding, as in the example of the 2 affected sisters from family MTP857, of whom one showed densely distributed deposits bilaterally in the whole fundus, whereas the other had very few deposits in the peripheral retina of only 1 eye. Thus, cases of RPA caused by *RLBP1* mutations might be underdiagnosed because of the absence or scarcity of the white dotlike deposits, in particular in children or in patients with late-stage disease.[16] These deposits are assumed to reflect the accumulation of all-*trans*-retinyl esters in the retinal pigment epithelium because impairment of cellular retinaldehyde-binding protein caused by *RLBP1* mutations slows down the process by which all-*trans*-retinyl esters are isomerized to 11-*cis*-retinol.[19] These deposits are also encountered in fundus albipunctatus due to *RDH5* mutations and in a few cases of retinal dystrophies due to *RPE65* mutations,[21] in which the visual cycle is impaired downstream from the retinyl esters. However, the deposits were also recently reported in a case patient with *LRAT* mutations,[22] in which no retinyl esters should be produced, indicating that their composition remains elusive.

Figure 5. Adaptive Optics–Based Infrared Fundus Ophthalmoscopy Images of the Parafoveal Area

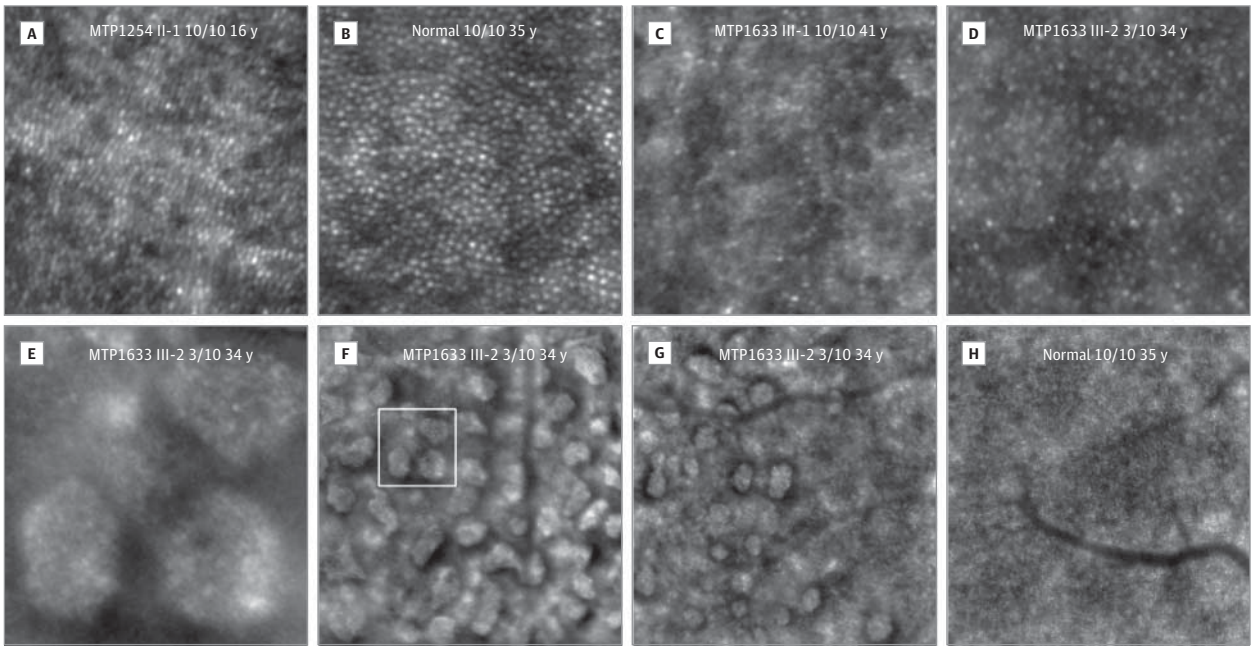

Family and patient numbers (or normal for control subjects), visual acuity, and age in years are indicated at the top of each image. A, C, and D, Patients have an abnormal cone mosaic. B, Control subject with a normal cone mosaic. E, White dotlike deposits. F, Visualization and magnification (white box) of the image in part E. G, No dotlike deposits are found in the fovea (right side of the picture). H, Similar area in a control.

Retinitis punctata albescens is a subtype of RP because progressive rod and cone cell death occurs with age. Nevertheless, we found that some variables of the disease progression, such as visual acuity, peripheral visual field, and cone ERG, were not correlated with age. This finding could be a result, in part, of relatively wide variations in the severity of the disease and also to the slow disease progression, so that the window of observation from ages 3 to 39 years was not sufficient to reveal a correlation in only 11 patients. The thickness of the macula outside the fovea was decreased, as observed in other forms of RP,[31] and this tended to worsen with age, indicating a slow progression of photoreceptor disorganization and death with time. In contrast, large variations in the foveal thickness were found, independent of age. Foveal thinning could be observed at early stages, as previously reported.[17] Such early foveal thinning has also been reported in patients with *RPE65* mutations, in which the same metabolism is impaired.[32] In addition, *Rpe65*$^{-/-}$ mice exhibit early cone degeneration.[33] This finding indicates that there is early cone death, and indeed cone mosaic disorganization and decrease in cone numbers were found in the patients of this study. Cone degeneration could be common to visual cycle impairment. Previous studies have found that cone opsins were mislocalized in *Rpe65*$^{-/-}$ mice[34,35] and that this could be restored by 11-*cis*-retinal[33,36] or 9-*cis*-retinal[37] supplementation. Therefore, depending on the degree of 11-*cis* availability, patients with RPA could undergo a variable degree of cone degeneration. In summary, RPA is initially detected as a slowly progressive retinal dystrophy with a variable degree of foveal cone death, even at an early stage. This finding has implications for future treatments.

ARTICLE INFORMATION

Submitted for Publication: November 24, 2012; final revision received March 14, 2013; accepted March 15, 2013.

Published Online: August 8, 2013. doi:10.1001/jamaophthalmol.2013.4476.

Author Affiliations: Genetics of Sensory Diseases, Centre Hospitalier Régional Universitaire de Montpellier, Montpellier, France (Dessalces, Meunier, Hamel); Institut des Neurosciences de Montpellier, Institut National de la Santé et de la Recherche Médicale (INSERM) U1051, Hôpital Saint-Eloi, Montpellier, France (Bocquet, Bourien, Meunier, Hamel); INSERM U1051, Université Montpellier 1, Montpellier, France (Bocquet, Bourien, Meunier, Hamel); INSERM U1051, Université Montpellier 2, Montpellier, France (Bocquet, Bourien, Meunier, Hamel); ElectroDiagnostic Imaging Unit, Low Vision Center, Clinique Sourdille, Nantes, France (Zanlonghi); currently in private practice, Avignon, France (Verdet).

Author Contributions: Ms Dessalces and Dr Hamel had full access to all the data in the study and take responsibility for the integrity of the data and the accuracy of the data analysis. Ms Dessalces and Dr Bocquet contributed equally to the manuscript.
Study concept and design: Bocquet, Meunier, Hamel.
Acquisition of data: Dessalces, Bocquet, Zanlonghi, Verdet, Meunier.
Analysis and interpretation of data: Bocquet, Bourien, Meunier, Hamel.
Drafting of the manuscript: Dessalces, Bocquet, Bourien, Meunier, Hamel.
Critical revision of the manuscript for important intellectual content: Zanlonghi, Verdet, Meunier, Hamel.
Statistical analysis: Bourien.
Obtained funding: Zanlonghi, Hamel.
Administrative, technical, and material support: Dessalces, Bocquet, Hamel.
Study supervision: Bocquet, Meunier, Hamel.

Conflict of Interest Disclosures: None reported.

Funding/Support: This study was supported by the Federation des Aveugles et Handicapés Visuels de France, Information Recherche sur la Rétinite Pigmentaire, Retina France, SOS Rétinite, and L'Union Nationale des Aveugles et Déficients Visuels. The foundation SOS Rétinite donated the OCT system and the AOIO camera.

Additional Contributions: We thank the patients and their families.

REFERENCES

1. Lauber H. Die Sogenannte retinitis punctata albescens. *Klin Monatsbl F Augenh*. 1910;48:133-148.

2. Banerjee BD, Das AB. Tapeto retinal degeneration (progressive retinitis punctata albescens) with anterior and posterior lenticonus (a case report). *Indian J Ophthalmol*. 1972;20(4):183-184.

3. Travkin AG, Basis VIu, Aladinskaia LV, Kunicheva GS. Hereditary association of tapeto-retinal dystrophy, retinitis punctata albescens, with spinal-cerebellar Friedreich's ataxia [in Russian]. *Vestn Oftalmol*. 1975;(3):84-87.

4. Fillastre JP, Guenel J, Riberi P, Marx P, Whitworth JA, Kunh JM. Senior-Loken syndrome (nephronophthisis and tapeto-retinal degeneration). *Clin Nephrol*. 1976;5(1):14-19.

5. Pearce WG, Gillan JG, Brosseau L. Bardet-Biedl syndrome and retinitis punctata albescens in an isolated northern Canadian community. *Can J Ophthalmol*. 1984;19(3):115-118.

6. Botelho PJ, Blinder KJ, Shahinfar S. Familial occurrence of retinitis punctata albescens and congenital sensorineural deafness. *Am J Ophthalmol*. 1999;128(2):246-247.

7. Maw MA, Kennedy B, Knight A, et al. Mutation of the gene encoding cellular retinaldehyde-binding protein in autosomal recessive retinitis pigmentosa. *Nat Genet*. 1997;17(2):198-200.

8. Burstedt MS, Sandgren O, Holmgren G, Forsman-Semb K. Bothnia dystrophy caused by mutations in the cellular retinaldehyde-binding protein gene (*RLBP1*) on chromosome 15q26. *Invest Ophthalmol Vis Sci*. 1999;40(5):995-1000.

9. Morimura H, Berson EL, Dryja TP. Recessive mutations in the *RLBP1* gene encoding cellular retinaldehyde-binding protein in a form of retinitis punctata albescens. *Invest Ophthalmol Vis Sci*. 1999;40(5):1000-1004.

10. Eichers ER, Green JS, Stockton DW, et al. Newfoundland rod-cone dystrophy, an early-onset retinal dystrophy, is caused by splice-junction mutations in *RLBP1*. *Am J Hum Genet*. 2002;70(4):955-964.

11. Scialfa A, Arnone G. Dominant retinitis pigmentosa and retinitis punctata albescens [in Italian]. *Ann Ottalmol Clin Ocul*. 1967;93(7):667-676.

12. Kajiwara K, Sandberg MA, Berson EL, Dryja TP. A *null* mutation in the human peripherin/RDS gene in a family with autosomal dominant retinitis punctata albescens. *Nat Genet*. 1993;3(3):208-212.

13. Souied E, Soubrane G, Benlian P, et al. Retinitis punctata albescens associated with the Arg135Trp mutation in the rhodopsin gene. *Am J Ophthalmol*. 1996;121(1):19-25.

14. Bocquet B, Lacroux A, Surget M-O, et al. Relative frequencies of inherited retinal dystrophies and optic neuropathies in Southern France. *Ophthalmic Epidemiol*. 2013;20(1):13-25.

15. Berson EL. Retinitis pigmentosa: the Friedenwald Lecture. *Invest Ophthalmol Vis Sci*. 1993;34(5):1659-1676.

16. Burstedt MS, Forsman-Semb K, Golovleva I, Janunger T, Wachtmeister L, Sandgren O. Ocular phenotype of Bothnia dystrophy: an autosomal recessive retinitis pigmentosa associated with an R234W mutation in the *RLBP1* gene. *Arch Ophthalmol*. 2001;119(2):260-267.

17. Burstedt MS, Golovleva I. Central retinal findings in Bothnia dystrophy caused by *RLBP1* sequence variation. *Arch Ophthalmol*. 2010;128(8):989-995.

18. Redmond TM, Yu S, Lee E, et al. *Rpe65* is necessary for production of 11-*cis*-vitamin A in the retinal visual cycle. *Nat Genet*. 1998;20(4):344-351.

19. Saari JC, Nawrot M, Kennedy BN, et al. Visual cycle impairment in cellular retinaldehyde binding protein (CRALBP) knockout mice results in delayed dark adaptation. *Neuron*. 2001;29(3):739-748.

20. Sparrow JR, Hicks D, Hamel CP. The retinal pigment epithelium in health and disease. *Curr Mol Med*. 2010;10(9):802-823.

21. Weleber RG, Michaelides M, Trzupek KM, Stover NB, Stone EM. The phenotype of Severe Early Childhood Onset Retinal Dystrophy (SECORD) from mutation of *RPE65* and differentiation from Leber congenital amaurosis. *Invest Ophthalmol Vis Sci*. 2011;52(1):292-302.

22. Littink KW, van Genderen MM, van Schooneveld M, et al. A homozygous frameshift mutation in LRAT causes retinitis punctata albescens. *Ophthalmology*. 2012;119(9):1899-1906.

23. Maguire AM, Simonelli F, Pierce EA, et al. Safety and efficacy of gene transfer for Leber's congenital amaurosis. *N Engl J Med*. 2008;358(21):2240-2248.

24. Bainbridge JW, Smith AJ, Barker SS, et al. Effect of gene therapy on visual function in Leber's congenital amaurosis. *N Engl J Med*. 2008;358(21):2231-2239.

25. Cideciyan AV, Aleman TS, Boye SL, et al. Human gene therapy for RPE65 isomerase deficiency activates the retinoid cycle of vision but with slow rod kinetics. *Proc Natl Acad Sci U S A*. 2008;105(39):15112-15117.

26. Humbert G, Delettre C, Sénéchal A, et al. Homozygous deletion related to Alu repeats in *RLBP1* causes retinitis punctata albescens. *Invest Ophthalmol Vis Sci*. 2006;47(11):4719-4724.

27. Marmor MF, Holder GE, Seeliger MW, Yamamoto S; International Society for Clinical Electrophysiology of Vision. Standard for clinical electroretinography (2004 update). *Doc Ophthalmol*. 2004;108(2):107-114.

28. Miller SA, Dykes DD, Polesky HF. A simple salting out procedure for extracting DNA from human nucleated cells. *Nucleic Acids Res*. 1988;16(3):1215.

29. Burstedt MS, Sandgren O, Golovleva I, Wachtmeister L. Effects of prolonged dark adaptation in patients with retinitis pigmentosa of Bothnia type: an electrophysiological study. *Doc Ophthalmol*. 2008;116(3):193-205.

30. Fishman GA, Roberts MF, Derlacki DJ, et al. Novel mutations in the cellular retinaldehyde-binding protein gene (*RLBP1*) associated with retinitis punctata albescens. *Arch Ophthalmol*. 2004;122(1):70-75.

31. Hood DC, Lin CE, Lazow MA, Locke KG, Zhang X, Birch DG. Thickness of receptor and post-receptor retinal layers in patients with retinitis pigmentosa measured with frequency-domain optical coherence tomography. *Invest Ophthalmol Vis Sci*. 2009;50(5):2328-2336.

32. Jacobson SG, Aleman TS, Cideciyan AV, et al. Defining the residual vision in Leber congenital amaurosis caused by *RPE65* mutations. *Invest Ophthalmol Vis Sci*. 2009;50(5):2368-2375.

33. Rohrer B, Lohr HR, Humphries P, Redmond TM, Seeliger MW, Crouch RK. Cone opsin mislocalization in *Rpe65*$^{-/-}$ mice. *Invest Ophthalmol Vis Sci*. 2005;46(10):3876-3882.

34. Samardzija M, Tanimoto N, Kostic C, et al. In conditions of limited chromophore supply rods entrap 11-*cis*-retinal leading to loss of cone function and cell death. *Hum Mol Genet*. 2009;18(7):1266-1275.

35. Zhang T, Zhang N, Baehr W, Fu Y. Cone opsin determines the time course of cone photoreceptor degeneration in Leber congenital amaurosis. *Proc Natl Acad Sci U S A*. 2011;108(21):8879-8884.

36. Zhang H, Fan J, Li S, et al. Trafficking of membrane-associated proteins to cone photoreceptor outer segments requires the chromophore 11-*cis*-retinal. *J Neurosci*. 2008;28(15):4008-4014.

37. Sato K, Ozaki T, Ishiguro S, Nakazawa M. M-opsin protein degradation is inhibited by MG-132 in *Rpe65*$^{-/-}$ retinal explant culture. *Mol Vis*. 2012;18:1516-1525.